Decadal-Scale Variation of South Asian Summer Monsoon Onset and Its Relationship with the Pacific Decadal Oscillation

TAKESHI WATANABE

Research and Information Center, Tokai University, Tokyo, Japan

KOJI YAMAZAKI

National Institute of Polar Research, Tachikawa, and Hokkaido University, Sapporo, Japan

(Manuscript received 4 September 2013, in final form 31 March 2014)

ABSTRACT

The variation of the summer monsoon onset over South Asia was investigated by using long-term data of the onset over Kerala, India, during the 64-yr period from 1948 to 2011. It was found that the onset over Kerala shows variation on a multidecadal scale. In early-onset years, the sea surface temperature (SST) anomaly over the northern Pacific Ocean was very similar to the negative Pacific decadal oscillation (PDO). The stationary wave train related to the negative PDO reaches into central Asia and generates a warm anomaly, thereby intensifying the land–sea thermal contrast, which promotes summer monsoon onset over South and Southeast Asia. The correlation between the onset date over Kerala and the PDO has strengthened since 1976. Analysis of zonal wind in the upper-level troposphere for the period 1958–2002 indicates that the change in the correlation is related to the change in the wave train path. The wave train propagating from the northern Pacific Ocean to western Russia could propagate eastward more easily in 1976–2002 than in 1958–75.

1. Introduction

The onset phase of the South Asian summer monsoon is characterized by an abrupt increase in precipitation and a development of low-level westerly and upper-level easterly wind. Because the variation of this monsoon has consequences for natural resources, such as water resources, renewable energy, and agricultural products, its onset is of great interest and importance.

The onset of the South Asian summer monsoon can be defined in several ways. Wang and LinHo (2002) defined the summer monsoon onset by using pentad-mean precipitation data reconstructed with the long-term mean and first 12 temporal harmonics. Their criterion for determining the summer monsoon onset date is that the reconstructed precipitation data exceeds 5 mm day^{-1} above the climatological January (July) mean in the Northern (Southern) Hemisphere. This simple and objective method enables discussion of the characteristics of global monsoon rainy seasons (Zhang and Wang 2008). The India Meteorological Department (IMD) annually determines the date of the summer monsoon onset over Kerala, a state in southwestern India. As mentioned by Joseph et al. (2006), the IMD used subjective estimates of wind field, precipitation, and humidity as criteria to determine monsoon onset before 2005. However, in 2006, the IMD shifted to an objective method that includes a criterion for outgoing longwave radiation. Fasullo and Webster (2003) determined the onset and withdrawal of the South Asian summer monsoon by using an index based on the hydrological cycle of areas affected by the South Asian monsoon. Their index is defined as the area average of vertically integrated moisture transport over the Arabian Sea. Joseph et al. (2006) proposed an objective method for determining monsoon onset over Kerala by using a combination of several criteria. Their method checks the structure and strength of the low-level westerly jet and convection. Although the precise date differs in some cases according to method used, these different methods adequately capture the summer monsoon onset.

Researchers have suggested that the advance of the South Asian summer monsoon onset in recent decades (Kajikawa et al. 2012; Kajikawa and Wang 2012; Xiang

Corresponding author address: T. Watanabe, Research and Information Center, Tokai University, 4-1-1 Kitakaname, Hiratsuka, Kanagawa, 259-1292, Japan.
E-mail: nabetake@ees.hokudai.ac.jp

DOI: 10.1175/JCLI-D-13-00541.1

and Wang 2013). Kajikawa et al. (2012) demonstrated the advanced onset of the monsoon over the Bay of Bengal and the western Pacific Ocean during the 30 years from 1979 to 2008, as determined using the method of Wang and LinHo (2002). They suggested that the advanced monsoon onset is due to intensification of thermal contrast between the Asian landmass and the tropical Indian Ocean in May, and is primarily caused by a warming trend over land. Kajikawa and Wang (2012) pointed out the advance of the summer monsoon onset over the South China Sea for the last 30 years. Xiang and Wang (2013) researched the mechanism of this advance through data analysis and a numerical experiment, and suggested that a shift to a La Niña–like mean state has promoted the advanced monsoon onset in recent decades. Whether such a trend can be observed before these three decades or for a longer term is an interesting question.

There have been some studies of long-term variation of the South Asian monsoon. Kumar et al. (1992) and Pal and Al-Tabbaa (2011) show long-term variation and change of seasonal- and monthly-mean precipitation over South Asia. Their results showed significant trends over some regions in India, but their results do not always agree, partly because the periods of their data differ. The recent study by Krishnamurthy and Krishnamurthy (2014) showed the relation between the strength of the South Asian summer monsoon and the Pacific decadal oscillation (PDO) using observed data and coupled numerical model data. They suggested that the warm (cold) phase of the PDO is associated with deficit (excess) rainfall over India in June–September and that the PDO modified the relationship between the Indian monsoon rainfall and El Niño–Southern Oscillation (ENSO). However, they did not discuss the variation of the summer monsoon onset. Previous studies have shown that the relation between the variation of the South Asian monsoon onset and ENSO is weak (e.g., Fasullo and Webster 2003; Adamson and Nash 2014). There is a need for more detailed investigation of the onset variability. For this purpose reliable long-term data are necessary, but only limited data are available.

In this study, we use long-term onset data from the IMD to investigate the variation of the summer monsoon onset over South Asia. We seek to answer three main questions: 1) What is the variation of the monsoon onset date over the long term? 2) How is the variation of the onset date related to variations in atmospheric circulation and SST? 3) What is the mechanism of such variation? We used monthly-mean reanalysis data and SST data to analyze large-scale atmospheric features so that synoptic-scale disturbance, which can function as a trigger for the onset, can be ignored (Krishnamurti et al. 1981).

This paper is organized as follows. Section 2 describes the data used. Section 3 discusses the variation of the monsoon onset over Kerala determined by the IMD and examines whether the monsoon onset over Kerala is related to the summer monsoon onset over other regions. Section 4 describes the meteorological mean state in relation to the variation of the onset over Kerala and shows a suggestive relationship between the onset over Kerala and the decadal-scale variation over the North Pacific Ocean. Section 5 discusses this relationship in detail. Section 6 is a discussion section. Section 7 summarizes this work.

2. Data

Our interest is in long-term variation of the South Asian summer monsoon onset. Long-term data of the onset date are necessary for this investigation, but only limited data are available. To compensate, we performed both statistical and meteorological analyses. Monthly-mean reanalysis and observational data were used to seek the mechanism for variation of the summer monsoon onset. We chose four datasets, listed below.

1) Monthly mean reanalysis data, provided by the 40-yr European Centre for Medium-Range Weather Forecasts (ECMWF) Re-Analysis (ERA-40; Uppala et al. 2005) on a 2.5° × 2.5° grid, were used for May and June in the period between 1958 and 2002. 2) The pentad mean of the Climate Prediction Center's (CPC) Merged Analysis of Precipitation (CMAP) data, on a 2.5° × 2.5° grid, was used for 1979–2010 (Xie and Arkin 1997). 3) The monthly-mean extended reconstructed SST provided by the National Oceanic and Atmospheric Administration (version v3b), on a 2° × 2° grid, was used for 1958–2002 (Smith et al. 2008). 4) The long-term record of the summer monsoon onset date from 1948 to 2011 as determined by the IMD was collected. The record from 1948 to 2003 was taken from Joseph et al. (2006) and the record from 2004 to 2011 was taken from the IMD's official web site. As mentioned in the introduction, the IMD's onset data have been researched and evaluated in previous studies. The long-term onset date determined by the IMD is thought to be useful and suitable for this study, although a few errors were discovered.

3. Summer monsoon onset over Kerala

First, we examined the long-term variation of the South Asian summer monsoon onset over Kerala (see rectangle, Fig. 2) provided by the IMD. Figure 1 shows time series of deviation of the onset date from the climatological data between 1948 and 2011. The median climatological onset date from 64 years of data is 31 May, and its standard

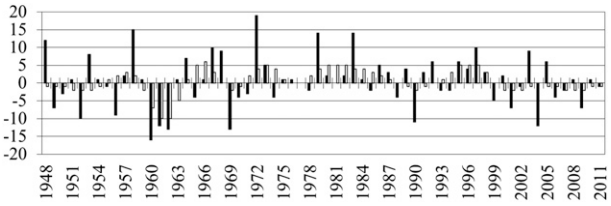

FIG. 1. Time series of the deviation of the IMD's monsoon onset date over Kerala from climatological data. The filled and unfilled bars represent the raw and the 6-yr low-pass-filtered time series, respectively. Positive and negative values indicate later and earlier onset than normal, respectively.

deviation is 7 days. Examining time series in only the most recent three decades, a trend toward early onset is identified, which is in agreement with previous studies (e.g., Kajikawa et al. 2012). However, the onset date is delayed from the 1960s to the 1970s. There are no long-term trends over the whole period. It is worth noting that the onset over Kerala shows variation on a multidecadal time scale. Early- and late-onset years were respectively defined as years when the onset date was 3 or more days earlier (before 29 May) or 3 or more days later (after 2 June) than the climatological onset date (31 May). A total of 20 early-onset years and 16 late-onset years are selected from among the years between 1948 and 2011 in the IMD onset (Tables 1 and 2).

To examine the extent to which the onset over Kerala is representative of the South Asian summer monsoon (i.e., whether it is related to the onset over other regions), we objectively determined the onset pentad date over Asia in early- and late-onset years over Kerala on the basis of CMAP pentad data following the method of Wang and LinHo (2002). Eleven early years and 10 late years were chosen between 1979 and 2010, the range for which pentad CMAP data are available [years marked with a plus sign (+) in Tables 1 and 2]. Two composites for pentad-mean precipitation were made for early- and late-onset years. Then, applying the method of Wang and LinHo (2002), the onset pentad date of the Asian monsoon in early- and late-onset years was determined. We mainly focused on areas where the climatological onset occurred within the May–June period (25th–36th pentads) (Fig. 2) because variations in such areas appeared to be closely related to the monsoon onset over Kerala.

TABLE 1. List of early-onset years. The plus signs (+) and asterisks (*) represent the year selected for compositing in section 3 and 4, respectively.

1960*	1961*	1962*	1965*
1969*	1970*	1971	1974
1978	1985^{+}	1988*$^{+}$	1990*$^{+}$
1993^{+}	1994^{+}	1999*$^{+}$	2001*$^{+}$
2004^{+}	2006^{+}	2007^{+}	2009^{+}

TABLE 2. List of late-onset years. The plus signs (+) and asterisks (*) represent the year selected for compositing in section 3 and 4, respectively.

1958*	1964*	1967*	1968*
1972*	1973	1979*$^{+}$	1983*$^{+}$
1986^{+}	1989^{+}	1992*$^{+}$	1995*$^{+}$
1996^{+}	1997*$^{+}$	2003^{+}	2005^{+}

The onset pentad and its anomaly for each grid when the onset over Kerala is early and late are shown in Figs. 3a and 3b, respectively. In early-onset years, the summer monsoon onset over the region from the southern Arabian Sea to southwestern India and over the region from the southern Bay of Bengal to the Indochina Peninsula is early. These two regions extend in the southwest–northeast direction. Earlier onset is also seen over the western North Pacific Ocean but, conversely, late onset is seen over southern China, Taiwan, and the northern Philippine Sea. In late-onset years, the variation of the onset over these regions shows an opposite sign (Fig. 3b). The onset over these regions varies in accordance with that over Kerala, and thus the onset over Kerala is representative for these regions (Fig. 3c).

The regional means of precipitation over the region from the Arabian Sea to southwestern India (7.5°–15.0°N, 60.0°–77.5°E) and Southeast Asia (10.0°–22.5°N, 97.5°–105.0°E) show an abrupt increase between mid-May and mid-June, and between late April and mid-May, respectively (Figs. 4a,b). The regional means of precipitation in Fig. 4a successfully show the difference of start-of-summer monsoon rainfall in early- and late-onset years, indicating that IMD onset is useful for the study and definition of early- and late-onset years.

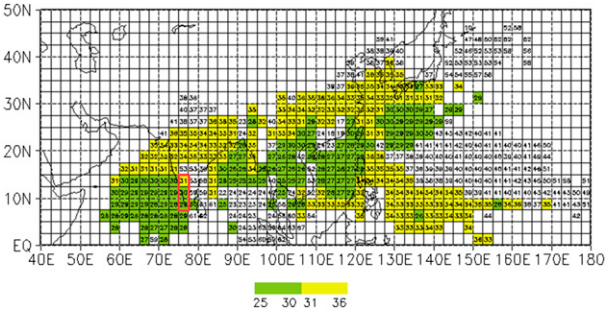

FIG. 2. Climatological onset pentad for the period between 1979 and 2011. Number represents the onset pentad date obtained using the method by Wang and LinHo (2002). Unnumbered grids indicate that the summer monsoon onset could not be determined. The red bold rectangle over the southwest Indian subcontinent corresponds to grids including the state of Kerala.

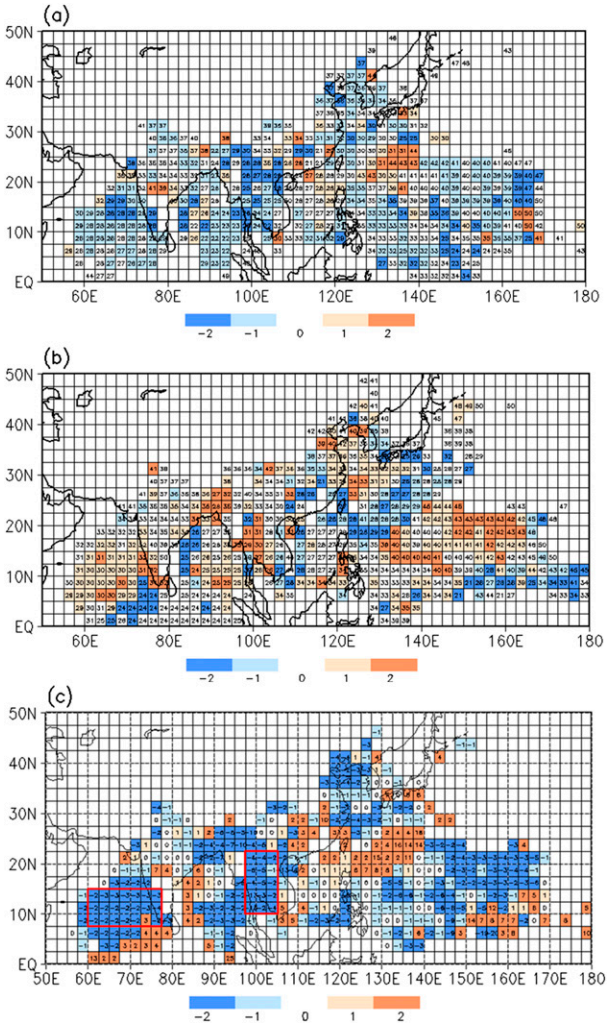

FIG. 3. Onset pentad for (a) the early-onset years and (b) the late-onset years. Shading indicates anomaly of the onset pentad date from climatology. (c) Difference in onset pentad date between the early- and late-onset years. Number shows the difference in the onset pentad date. The red bold rectangles over the region from the Arabian Sea to the southwest Indian subcontinent and Southeast Asia indicate regions where the regional mean precipitation in Fig. 4 is defined.

The monthly- and seasonal-mean precipitation averaged over the region from the Arabian Sea to the southwestern Indian subcontinent and over Southeast Asia are summarized in Tables 3 and 4. Precipitation in May of early-onset years is greater than that of late-onset years over both regions, but the difference over Southeast Asia is not significant with 95% confidence. Differences of seasonal-mean (May–September) precipitation are not confirmed over either region, which indicates that the timing of the summer monsoon onset is not associated with the intensity of precipitation in the summer monsoon season over these regions.

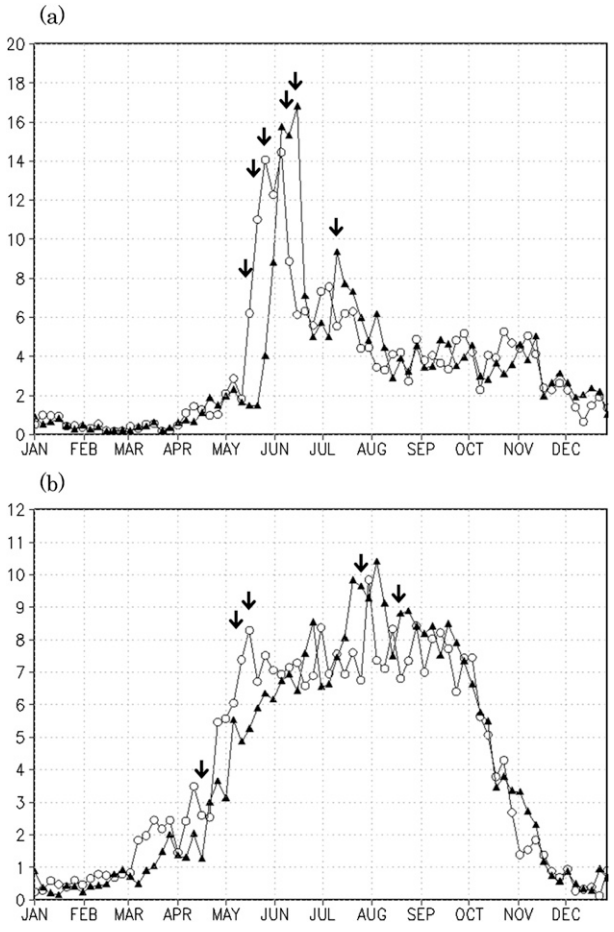

FIG. 4. Time series of the regional mean of pentad-mean precipitation (mm day^{-1}) over (a) the region from the Arabian Sea to the southwest Indian subcontinent (7.5°–15°N, 60°–77.5°E) and (b) Southeast Asia (10.0°–22.5°N, 97.5°–105.0°E). Circles and triangles indicate early- and late-onset years, respectively. Arrows indicate pentad dates where the difference between early- and late-onset years is significant with 95% confidence.

4. Atmospheric and oceanic states related to the variation of the onset over Kerala

To find the mechanism of the variation of the onset, we investigated the mean state's relationship with the variation of the Kerala onset using composite analysis. The 10

TABLE 3. Monthly-mean precipitation (mm day^{-1}) over the region from the Arabian Sea to the southwestern Indian subcontinent. The asterisk (*) indicates that the difference between early- and late-onset years is significant with 95% confidence.

	May	June	July	August	September	May–September
Early years	6.3*	8.9	6.2	3.9	4.1	5.9
Late years	2.1*	11.4	6.8	4.3	4.0	5.7

TABLE 4. Monthly-mean precipitation (mm day^{-1}) over Southeast Asia. Differences of all monthly and seasonal means between early- and late-onset years are not significant ($p \geq 0.05$).

	May	June	July	August	September	May–September
Early years	6.9	7.0	7.4	7.9	7.5	7.3
Late years	5.2	7.1	8.0	8.9	8.0	7.4

earliest-onset and 10 latest-onset years over Kerala were chosen between 1958 and 2002 [years marked with an asterisk (*) in Tables 1 and 2]. Then, composites were made for various fields. As the climatological onset over Kerala is 31 May we examined the monthly mean state in May and June.

Figures 5a and 5b show composites for horizontal wind at 850 hPa in May in early- and late-onset years, respectively. The westerly over the northern Indian Ocean between 5° and 10°N in early-onset years is stronger than that in late-onset years and is located over the southern Indian subcontinent, including Kerala. The difference is shown in Fig. 5c. Cyclonic circulation anomalies are seen over the Arabian Sea and the Bay of Bengal. Southwesterlies accompanied by anomalous circulation intensify water vapor transport from the Arabian Sea to the Indian subcontinent and from the Bay of Bengal to Indochina. These regions correspond with the earlier-onset regions in early-onset years, as seen in Fig. 3. The early establishment of monsoon westerlies over the northern Indian Ocean is related to the early onset of the summer monsoon over Southeast and South Asia. Figure 5d shows the composite difference for horizontal wind at 850 hPa in June, showing the anomalous westerlies from the Arabian Sea to the Philippines.

Global atmospheric circulation anomalies related to the timing of onset of the South Asian summer monsoon were examined. Figure 6 shows the composite difference in geopotential height at 300 hPa in May, as well as wave activity flux (Takaya and Nakamura 2001). The figure shows a stationary wave train from the northern Pacific Ocean to central Asia (from the Iranian Plateau to the western Tibetan Plateau), which generates an anticyclonic anomaly over central Asia.

To examine the tropospheric temperature, the composite difference of thickness between 300 and 500 hPa and the surface temperature in May are shown in Fig. 7. A positive-temperature anomaly is seen over central Asia. This warm anomaly causes a strong land–sea thermal contrast, which likely promotes summer monsoon onset over South and Southeast Asia. The warm temperature anomaly from the upper troposphere to the surface is generated by the anticyclonic anomaly over central Asia (Zhang et al. 2004; Tamura et al. 2010; Watanabe and Yamazaki 2012).

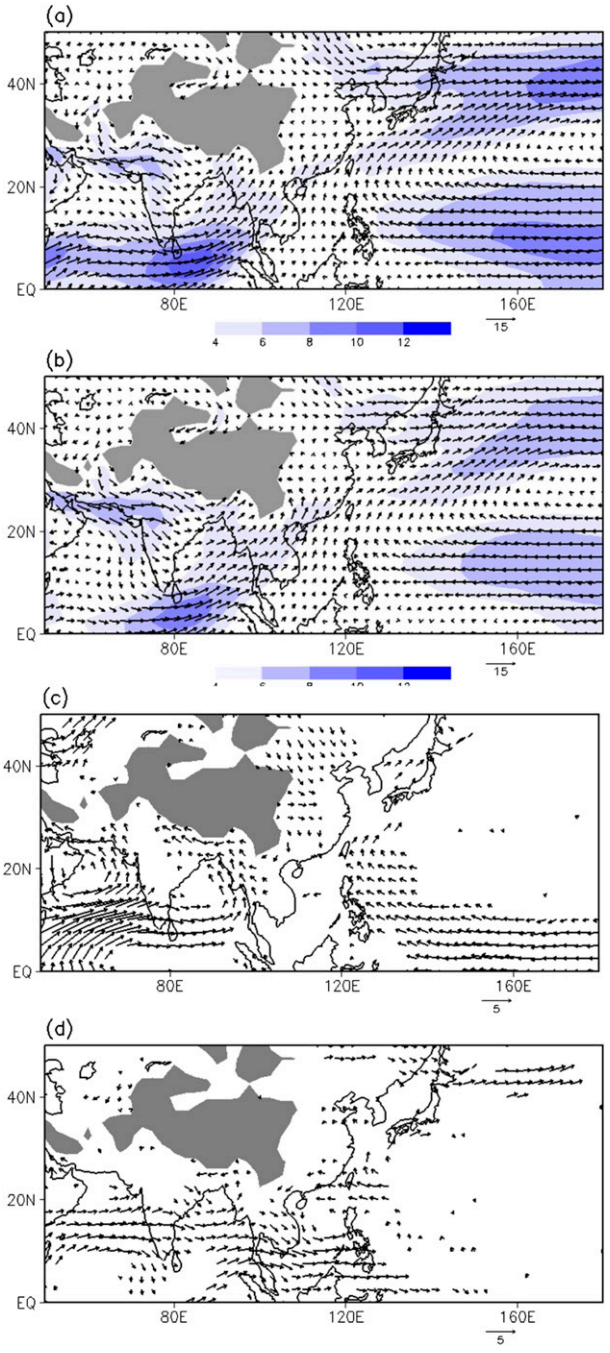

FIG. 5. Composite related with variation of the onset for horizontal wind at 850 hPa in May in (a) early-onset years and (b) late-onset years. Arrows represent horizontal wind vectors (m s^{-1}). Shading indicates horizontal wind speed (m s^{-1}). Also shown is the composite difference of horizontal wind (m s^{-1}) at 850 hPa in (c) May and (d) June. The composite difference is defined as the composite for early-onset years minus that of late-onset years. An arrow is plotted on the grid where the difference is confident at the 95% level.

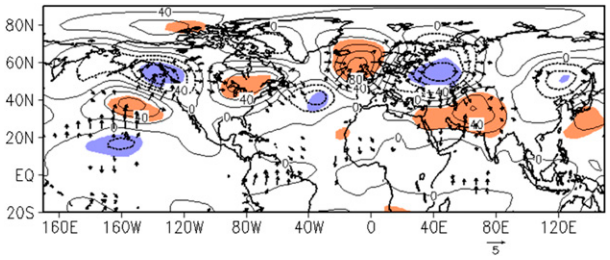

FIG. 6. As in Fig. 5c, but for geopotential height at 300 hPa in May. The contour interval is 20 m. Color shading indicates that the difference (orange, positive; blue, negative) is statistically significant with 95% confidence. Arrows represent wave activity flux calculated from composite difference for streamfunction and are plotted at only grid cells where magnitude is greater than 1 $m^2 s^{-2}$.

To visualize divergent wind field–related convective activity on a large scale, the composite difference of velocity potential and associated divergent wind field at 300 and 850 hPa in May are shown in Fig. 8. The difference indicates enhanced convection over South and Southeast Asia in May, and its maximum is around the region from the Arabian Sea to the southwest Indian subcontinent. The enhanced convection seems to be related to an earlier start-of-summer monsoon rainfall over the region (Figs. 3 and 4). The upper-level divergent wind coincides with convergence over central Asia and the Arabian Peninsula. This result is in agreement with previous studies (Rodwell and Hoskins 1996; Hsu et al. 1999; Zhang et al. 2004; Tamura et al. 2010). Watanabe and Yamazaki (2014) showed that heating in the middle troposphere over the northern Indian Ocean (centered at 5°N, 90°E) generates an anticyclonic anomaly over central Asia in May–June by a numerical experiment using the linear baroclinic model. The anticyclonic anomaly over central Asia, as seen in Fig. 6, appears to be related not only to the stationary wave train in the middle latitudes but also to strong convection over South and Southeast Asia. It seems that anomalous convection related to the timing of the onset feeds back into the development of the anticyclonic anomaly over central Asia.

The composite difference of near-surface temperature shows an interesting distribution over the northern and tropical Pacific Ocean (Fig. 7b). A high-temperature anomaly is seen over the middle and the western part of the North Pacific Ocean and a negative-temperature anomaly is seen over the eastern part of the North Pacific Ocean in early-onset years. At the same time, a negative-temperature anomaly is seen over the central region of the tropical Pacific Ocean. This distribution over the northern Pacific Ocean is similar to that seen in the negative phase of the PDO (Mantua and Hare 2002). The composite difference for SST in May shows negative PDO-like distribution over the northern Pacific Ocean

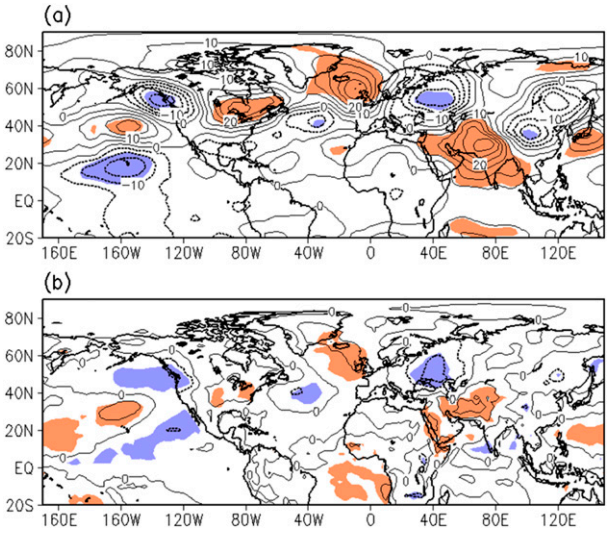

FIG. 7. (a) As in Fig. 5c, but for thickness between 300 and 500 hPa in May. Contour interval is 5 m. (b) As in Fig. 5c, but for temperature at a height of 2 m in May. Contour interval is 1 K. Color shading indicates that the difference (orange, positive; blue, negative) is statistically significant with 95% confidence.

(Fig. 9b) as well. This negative PDO-like distribution is also seen in April and June, even in winter (January–March; not shown). The SST anomaly over the tropical Pacific Ocean in early-onset years corresponds to a La Niña pattern, which agrees with the findings by Fasullo

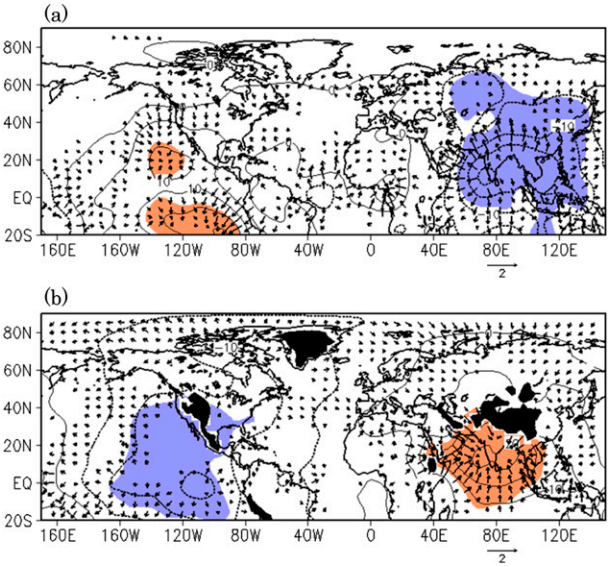

FIG. 8. As in Fig. 5c, but for velocity potential at (a) 300 and (b) 850 hPa in May. Contour interval is 5×10^5 $m^2 s^{-1}$. Color shading indicates that the difference (orange, positive; blue, negative) is statistically significant with 95% confidence. Arrows represent divergent wind, and are plotted at only grid cells where the magnitude exceeds 0.2 $m s^{-1}$.

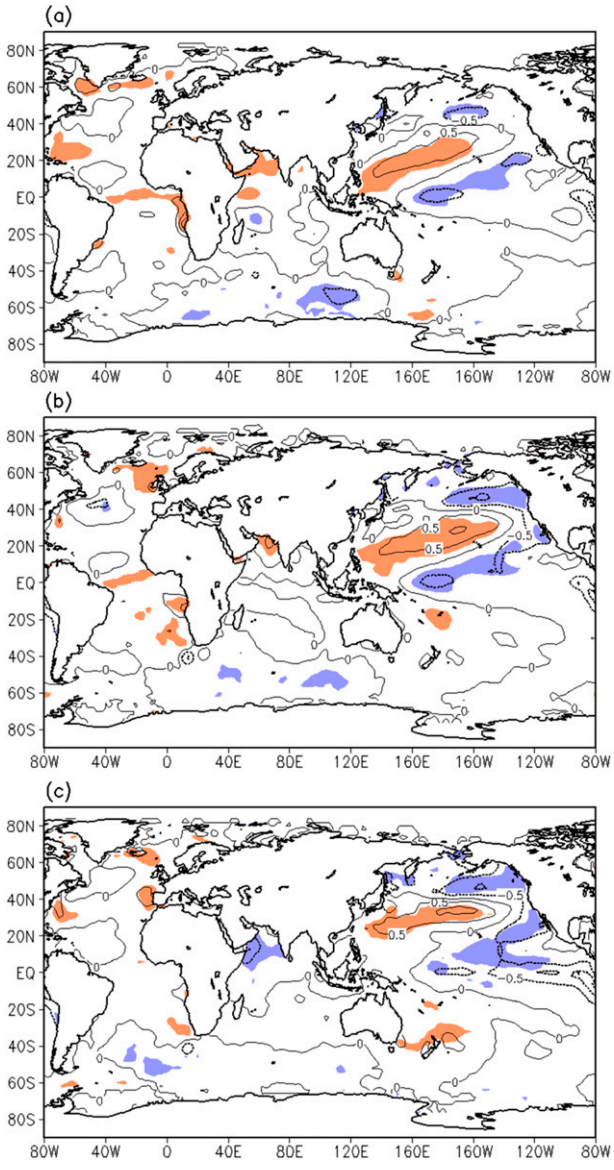

FIG. 9. (a) As in Fig. 5c, but for sea surface temperature in (a) April, (b) May, and (c) June. Contour interval is 0.5 K. Color shading indicates that the difference (orange, positive; blue, negative) is statistically significant with 95% confidence.

and Webster (2003). This suggests that the PDO and ENSO control the timing of the South Asian summer monsoon onset. Results of composite analysis related with IMD onset suggest a relation between the variation of monthly-mean SST over the North Pacific Ocean and variation of circulations over Asian monsoon regions.

In addition to PDO- and La Niña–like patterns, a warm SST anomaly is seen over the northern Arabian Sea in April and May (Fig. 9). Together with the warm anomaly over central Asia and the surrounding land area (Fig. 7), this warm SST enhances north–south temperature contrasts in early-onset years. This enhanced heat contrast causes the early onset. After the onset (i.e., in June) (Fig. 9c), the SST in the northern Arabian Sea becomes cooler, probably because strong low-level winds (Fig. 5) enhance oceanic evaporative cooling.

Judging comprehensively from the results of composite analysis related with IMD onset, it is thought that variation of the SST over the North Pacific Ocean influences summer monsoon onset over South Asia, and that the stationary wave train plays an active role in connecting both regions. This raises the following question: How are the PDO and La Niña related to the monsoon onset? In the next section, we focus on these relationships and their possible cause.

5. Relationship between the PDO and monsoon onset over Kerala

The PDO is the interdecadal variability observed in the northern Pacific Ocean and shows two periodicities: 15–25 and 50–70 yr. The PDO index is defined as the leading principal component of monthly-mean SST over the North Pacific Ocean (Mantua and Hare 2002). The positive PDO index represents the warm phase when a cold SST anomaly is seen over the central North Pacific and a warm SST anomaly is seen along the eastern North Pacific; the negative PDO index represents the opposite distribution. The PDO index used in this study was obtained from the Joint Institute for the Study of the Atmosphere and Ocean (http://jisao.washington.edu/pdo/).

Figure 10a shows the time series of the PDO index for the period 1948–2011, together with the onset date anomaly over Kerala from the climate data shown in Fig. 1a. Figure 10b shows the same data, but using 6-yr low-pass-filtered data (Duchon 1979). The PDO index is a 3-month average from March to May. The correlation between the PDO index and the monsoon onset date at Kerala for the 64-yr span is +0.199, which is not statistically significant at the 90% confidence. However, since 1976, the periods and phases of the two time series coincide well. The correlation coefficients are −0.038 for the period from 1948 to 1975 and +0.410 for the period from 1976 to 2011. The +0.410 value of the correlation coefficient for the recent period is statistically significant at the 98% confidence.

The 30-yr moving correlation coefficients between the PDO index and monsoon onset date rapidly increase after about 1973 and become about +0.4 after 1976 (Fig. 11). A considerable negative correlation is seen in some years before 1975, such as in 1966 and 1972, and no correlation is observed before 1975. However, an abrupt increase of the 30-yr moving correlation coefficient is seen following 1976. This suggests that the advance of monsoon onset

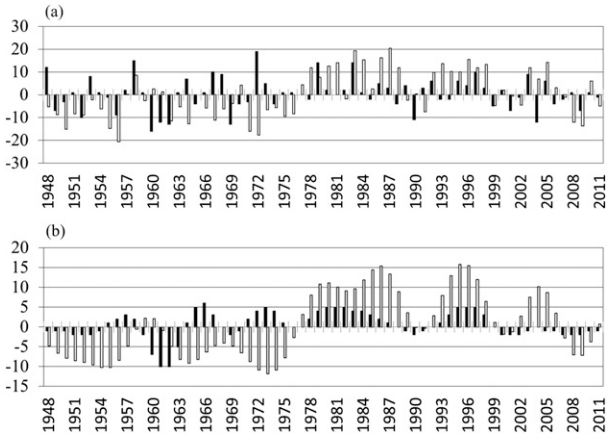

FIG. 10. (a) Raw and (b) 6-yr-filtered time series of the PDO index together with anomaly of onset date over Kerala shown in Fig. 1. Unfilled and filled bars correspond to the PDO index multiplied by 10 and deviation of the onset date, respectively. The PDO index is scaled for convenience to compare both time series.

over the Arabian Sea and the Bay of Bengal in recent decades is related to the multidecadal variation caused by the PDO.

The relationship between the monsoon onset and ENSO was also examined using the SST anomaly data over the Niño-3 region (not shown). The 30-yr moving correlation coefficients between SST over the Niño-3 region and monsoon onset date increased after around 1970, which is statistically significant with 95% confidence, but some correlation coefficients are only marginally significant. Although the summer monsoon onset has become more closely related to both the PDO and ENSO in recent decades, this increase of correlation between the monsoon onset and the PDO is noticeably abrupt.

We investigated why the relationship between the monsoon onset over Kerala and the PDO changes before and after 1975 using composites for both separate periods. The earlier period was defined as the 18 years from 1958 to 1975, and the later period was the 27 years from 1976 to 2002. The one-third highest and the one-third lowest PDO index years based on 6-yr low-pass-filtered data, shown in Fig. 10b, were selected separately for both periods. As a result, 6 positive and 6 negative PDO years were selected from the earlier period, and 9 positive and 9 negative PDO years were selected from the later period. Then, composites were made in each period separately. Note that the average PDO index in the earlier period is mostly negative and in the later period is mostly positive.

To examine the upper-level circulation pattern and wave propagation associated with the PDO, the composite difference in 300-hPa geopotential height between positive and negative PDO years for each period is shown

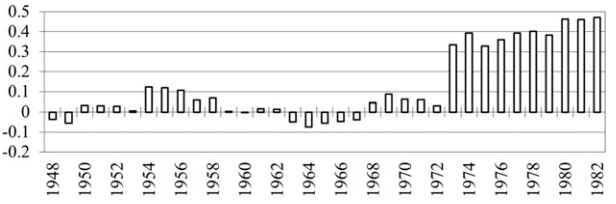

FIG. 11. 30-yr moving correlation coefficient between the PDO index and the onset date over Kerala. Horizontal axis represents the starting year of each 30-yr period.

in Fig. 12, together with wave activity flux. The wave train propagates from the North Pacific Ocean to Greenland and generates an anticyclonic anomaly on the positive PDO phase in both periods (Fig. 12). However, paths and intensities of wave trains in both periods diverged at a point downstream from Greenland. The wave train in the earlier period propagated southeastward and generated another anticyclonic anomaly over the Black Sea (40°N, 40°E), but did not clearly propagate farther downstream (Fig. 12a). In contrast, during the later period, the wave train propagated eastward, reaching into western Russia (55°N, 50°E) (Fig. 12b), after which it tended to propagate southeastward and eastward. As a result, the

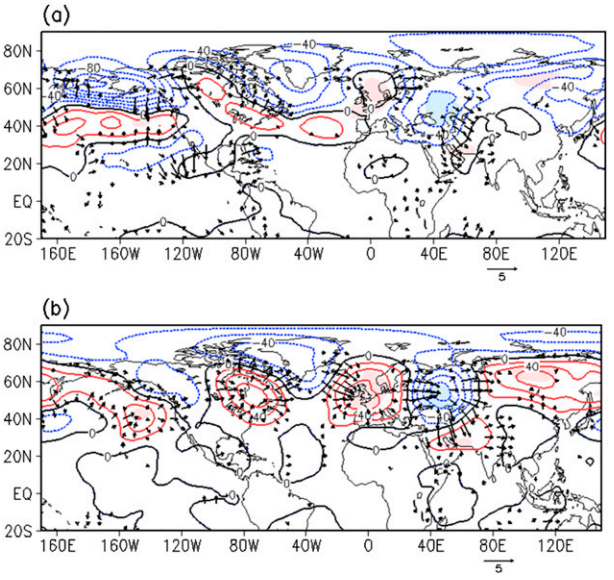

FIG. 12. Composite difference related with the PDO of geopotential height at 300 hPa between positive and negative PDO years for (a) the earlier period from 1958 to 1975 and (b) the later period from 1976 to 2002. The composite difference is defined as the negative PDO composite minus the positive PDO composite. The contour interval is 10 m. Color shading indicates that the difference (orange, positive; blue, negative) is statistically significant with 95% confidence. Arrows indicate wave activity flux ($m^2 s^{-2}$) calculated from the composite difference of the streamfunction at 300 hPa, and are plotted at only grid cells where the magnitude exceeds 1 $m^2 s^{-2}$.

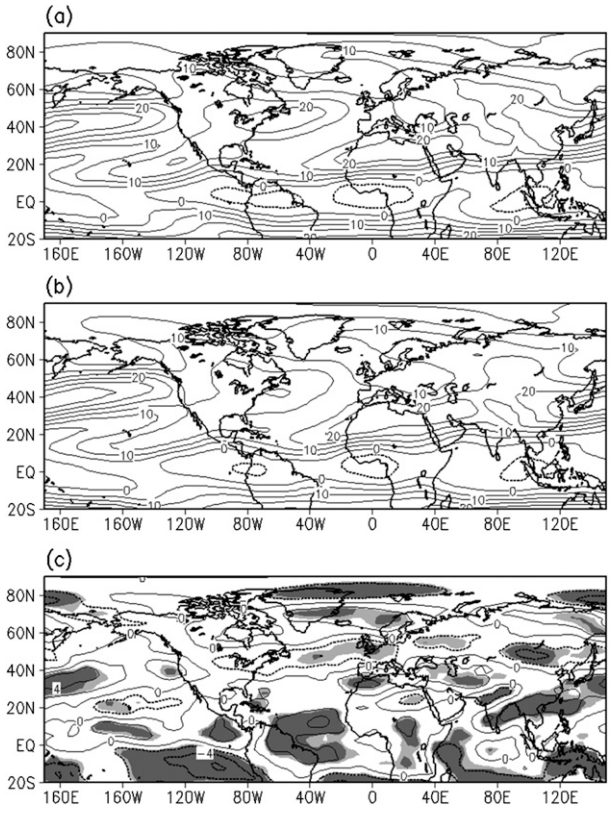

FIG. 13. (a) Climatological data on zonal wind at 300 hPa for (a) the earlier period from 1958 to 1975 and (b) the later period from 1976 to 2002. Contour interval is 10 m s^{-1}. (c) Difference of climatological data on zonal wind at 300 hPa between the earlier period and the later period. Contour interval is 2 m s^{-1}. Dark and light gray colors indicate difference is statistical significance with the 95% and 90% confidence, respectively.

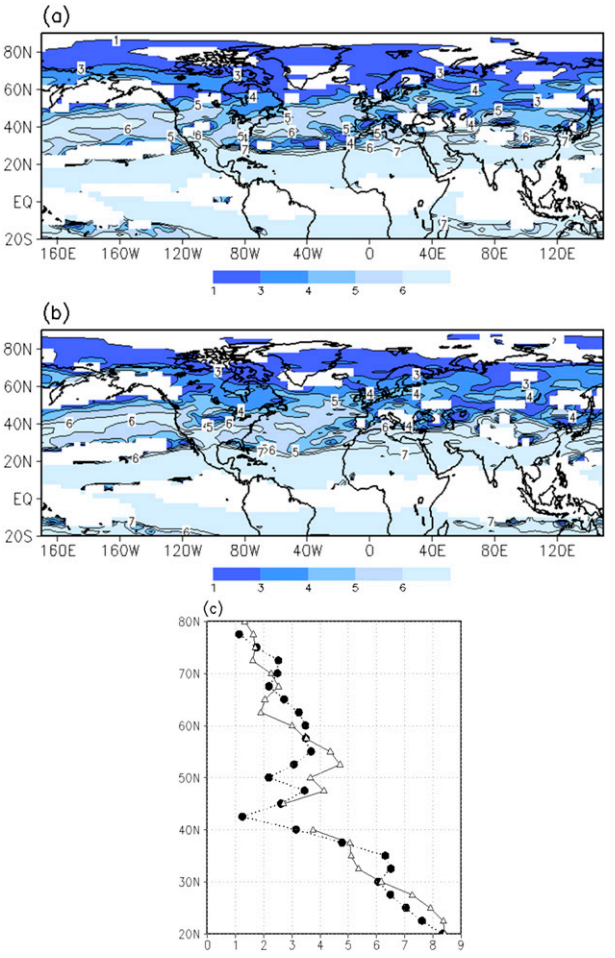

FIG. 14. Wavenumber of stationary Rossby waves at 300 hPa for (a) the earlier period 1958 to 1975 and (b) the later period 1976 to 2002. The white grid is where the stationary Rossby wave is not defined. (c) Wavenumber calculated from zonal-mean zonal wind at 300 hPa from 20°W to 60°E for the earlier period (solid line with triangle) and the later period (dotted line with circle). Line breaks indicate that the wavenumber is undefined at that latitude.

negative (positive) geopotential anomalies were generated over central Asia during the positive (negative) PDO phase. The strength of this anomalous geopotential height in the later period was stronger than that in the earlier period, which is assumed to partially reflect the difference of propagation of the wave activity.

We speculate that the different atmospheric responses to the PDO between earlier and later periods are due to their different mean flows (Fig. 12). Figure 13 shows 300-hPa zonal winds for each period and their differences. Zonal wind speeds at 300 hPa in both periods differed between the northern Atlantic Ocean and the Eurasian continent. The westerly wind is weaker around 55°N and stronger between northern Africa and central Asia along 40°N in the later period. Applying the Rossby ray path theory (Hoskins and Ambrizzi 1993), Rossby waveguides in two periods are compared. The wavenumber of the stationary Rossby wave was calculated from the mean state in each period (Fig. 14), revealing the difference in Rossby waveguides between periods. The waveguide from Europe to western Russia was narrow in the early period but broader in the later period (Figs. 14a,b). Figure 14c shows the difference clearly. The distribution of wavenumber centered at 60°N between 50° and 67.5°N in the later period is typical of the waveguide. The stationary Rossby wave, whose wavenumber is 3 or 4, tends to be trapped in this waveguide. In contrast, the waveguide is confined to the narrow area centered at 52.5°N in the earlier period. Additionally the wavenumber around 42.5°N is not defined. The stationary Rossby wave is difficult to maintain there in the earlier period.

6. Discussion

In this study, we identified a relation between the Asian summer monsoon onset and the PDO by data analysis,

and a mechanism for such a relation. However, many questions and considerations remain.

The present study focused on the influence of wave trains through the subtropics, associated with the PDO on the summer monsoon onset, but the South Asian monsoon onset seems to be related to other variations over the tropical Pacific, the northern Indian Ocean, and the South China Sea. The relation to SST variations over the tropical Pacific and the northern Indian Ocean are mentioned briefly in sections 4 and 5. Some studies showed a relation between summer monsoons over South Asia and over the South China Sea (Hsu et al. 1999; Zhang et al. 2004), emphasizing a relation between the onset over the Bay of Bengal and over the South China Sea. Figures 3c and 5c, which are related to the variation of the onset over Kerala, do not show significant signals over the South China Sea. This suggests that monsoon onset over western South Asia is not directly related to monsoons over the South China Sea.

We showed one reason for the change in atmospheric responses to the PDO in section 5 by using the Rossby ray path theory. As mentioned by Hoskins and Ambrizzi (1993), waves of all wavenumber are reflected over the area where the wavenumber is not defined. However, some researchers have shown wave trains propagating from Europe and western Russia into the Asian subtropical jet through undefined areas (i.e., areas with an undefined wavenumber) over central Asia (Hoskins and Ambrizzi 1993; Ambrizzi et al. 1995; Ding and Wang 2005; Watanabe and Yamazaki 2014). The undefined areas are seen around the Black Sea and Caspian Sea in both periods (Fig. 14). The undefined area in the earlier period is thicker and broader; by comparison, the undefined area in the later period is thinner and had some openings, so the Rossby wave could easily penetrate or leak southeastward toward central Asia. The waveguides in both periods agree well with the directions indicated by wave activity (Fig. 12). It is suggested that difficulty in propagation of the wave train through central Asia modulates the relation between the South Asian monsoon and the PDO, although details of the mechanisms remain unclear.

The trend toward early onset over the past three decades seems to be related to the shift from positive to negative PDO (Fig. 10), but we could not judge whether the trend in recent decades is significant because periods of data used in this study are equal to one or two PDO cycles. Interesting open questions include whether there is a relation between summer monsoon onset and the PDO in longer-term data, and whether the signals of decadal-scale variation and any trend toward early onset can be separated out. It is also unclear what processes are responsible for the mean climatic zonal flow change that occurred in the mid-1970s, where the low-frequency PDO (50-yr time scale) changed from negative to positive. Is there any possibility that a strong PDO–monsoon onset relationship exists for only the positive phase of the PDO, and will this relationship continue in the future? How and to what extent does global warming play a role in the change of the PDO–onset relationship, or in the recent advancing trend of South Asian summer monsoon onset? These subjects are beyond the scope of the present paper and should be studied in the future.

7. Summary

We investigated the variation of the South Asian summer monsoon onset for 1948–2011 by using the long-term onset data over Kerala, India. We found that decadal-scale variation of South Asian summer monsoon onset is related to the PDO, and that the relation has strengthened over the past three decades. Our conclusions are listed below.

1) The monsoon onset date shows a trend toward early onset in the most recent three decades, although the trend is not recognized over a long-term period. It is worth noting that the monsoon onset shows variation on a multidecadal time scale.
2) With regard to early-onset years over Kerala, the summer monsoon onset was early over the following regions: the region from the southern Arabian Sea to southwestern India, the region from the southern Bay of Bengal to the Indochina Peninsula, and the western North Pacific Ocean. On the other hand, the onset was late over southern China, Taiwan, and the northern Philippine Sea.
3) The low-level westerly was strengthened in early-onset years. At the same time, the stationary wave train was located in the northern Pacific Ocean to central Asia and induced formation of an anticyclonic anomaly over central Asia. The stationary wave train is related to the variation of SST in the Pacific Ocean. A warm anomaly from the upper troposphere to the surface was generated by the anticyclonic anomaly and intensified thermal contrast between land and sea. The land–sea thermal contrast over central Asia promoted the summer monsoon onset over South and Southeast Asia.
4) The negative PDO- and La Niña–like distribution of SST anomaly appeared in early-onset years. In contrast, a similar distribution but with opposite sign is seen in late-onset years. Although the correlation coefficient between the monsoon onset over Kerala and the PDO from 1948 to 2011 is not statistically significant, the relationship strengthens after 1976. The 30-yr moving correlation coefficient abruptly increases around 1976 and reaches about +0.4 after 1976. The correlation between the onset over Kerala and the SST

anomaly over the Niño-3 region also increased after about 1970.

5) The change of the relationship between the monsoon onset over Kerala and the PDO seemed to be related to the change of path of the wave train. Through analysis of the Rossby waveguide in the period 1958 to 2002, it was found that the wave train could propagate eastward and southeastward over western Russia more easily in the period 1976–2002 than in the period 1958–1975.

Acknowledgments. We thank three anonymous reviewers for their constructive comments. This study was partly supported by the "Green Network of Excellence" Program (GRENE Program) Arctic Climate Change Research Project, Japan, and the Japan Science and Technology Agency (JST)/CREST/EMS/TEEDDA.

REFERENCES

Adamson, G. C. D., and D. J. Nash, 2014: Documentary reconstruction of monsoon rainfall variability over western India, 1781–1860. *Climate Dyn.,* **42,** 749–769, doi:10.1007/s00382-013-1825-6.

Ambrizzi, T., B. J. Hoskins, and H.-H. Hsu, 1995: Rossby wave propagation and teleconnection patterns in the austral winter. *J. Atmos. Sci.,* **52,** 3661–3672, doi:10.1175/1520-0469(1995)052<3661:RWPATP>2.0.CO;2.

Ding, Q., and B. Wang, 2005: Circumglobal teleconnection in the Northern Hemisphere summer. *J. Climate,* **18,** 3483–3505, doi:10.1175/JCLI3473.1.

Duchon, C. E., 1979: Lanczos filtering in one and two dimensions. *J. Appl. Meteor.,* **18,** 1016–1022, doi:10.1175/1520-0450(1979)018<1016:LFIOAT>2.0.CO;2.

Fasullo, J., and P. J. Webster, 2003: A hydrological definition of Indian monsoon onset and withdrawal. *J. Climate,* **16,** 3200–3211, doi:10.1175/1520-0442(2003)016<3200a:AHDOIM>2.0.CO;2.

Hoskins, B. J., and T. Ambrizzi, 1993: Rossby wave propagation on a realistic longitudinally varying flow. *J. Atmos. Sci.,* **50,** 1661–1671, doi:10.1175/1520-0469(1993)050<1661:RWPOAR>2.0.CO;2.

Hsu, H.-H., C.-T. Terng, and C.-T. Chen, 1999: Evolution of large-scale circulation and heating during the first transition of Asian summer monsoon. *J. Climate,* **12,** 793–810, doi:10.1175/1520-0442(1999)012<0793:EOLSCA>2.0.CO;2.

Joseph, P. V., K. P. Sooraj, and C. K. Rajan, 2006: The summer monsoon onset process over South Asia and an objective method for the date of monsoon onset over Kerala. *Int. J. Climatol.,* **26,** 1871–1893, doi:10.1002/joc.1340.

Kajikawa, Y., and B. Wang, 2012: Interdecadal change of the South China Sea summer monsoon onset. *J. Climate,* **25,** 3207–3218, doi:10.1175/JCLI-D-11-00207.1.

——, T. Yasunari, S. Yoshida, and H. Fujinami, 2012: Advanced Asian summer monsoon onset in recent decades. *Geophys. Res. Lett.,* **39,** L03803, doi:10.1029/2011GL050540.

Krishnamurthy, L., and V. Krishnamurthy, 2014: Decadal scale oscillations and trend in the Indian monsoon rainfall. *Climate Dyn.,* doi:10.1007/s00382-013-1870-1, in press.

Krishnamurti, T. N., P. Ardanuy, Y. Ramanathan, and R. Pasch, 1981: On the onset vortex of the summer monsoon. *Mon. Wea. Rev.,* **109,** 344–363, doi:10.1175/1520-0493(1981)109<0344:OTOVOT>2.0.CO;2.

Kumar, K. R., G. B. Pant, B. Parthasarathy, and N. A. Sontakke, 1992: Spatial and subseasonal patterns of the long-term trends of Indian summer monsoon rainfall. *Int. J. Climatol.,* **12,** 257–268, doi:10.1002/joc.3370120303.

Mantua, N. J., and S. R. Hare, 2002: The Pacific decadal oscillation. *Oceanography,* **58,** 35–44, doi:10.1023/A:1015820616384.

Pal, I., and A. Al-Tabbaa, 2011: Assessing seasonal precipitation trends in India using parametric and non-parametric statistical techniques. *Theor. Appl. Climatol.,* **103,** 1–11, doi:10.1007/s00704-010-0277-8.

Rodwell, M. J., and B. J. Hoskins, 1996: Monsoons and the dynamics of deserts. *Quart. J. Roy. Meteor. Soc.,* **122,** 1385–1404, doi:10.1002/qj.49712253408.

Smith, T. M., R. W. Reynolds, T. C. Peterson, and J. Lawrimore, 2008: Improvements to NOAA's Historical Merged Land–Ocean Surface Temperature Analysis (1880–2006). *J. Climate,* **21,** 2283–2296, doi:10.1175/2007JCLI2100.1.

Takaya, K., and H. Nakamura, 2001: A formulation of a phase-independent wave-activity flux for stationary and migratory quasigeostrophic eddies on a zonally varying basic flow. *J. Atmos. Sci.,* **58,** 608–627, doi:10.1175/1520-0469(2001)058<0608:AFOAPI>2.0.CO;2.

Tamura, T., K. Taniguchi, and T. Koike, 2010: Mechanism of upper tropospheric warming around the Tibetan Plateau at the onset phase of the Asian summer monsoon. *J. Geophys. Res.,* **115,** D02106, doi:10.1029/2008JD011678.

Uppala, S. M., and Coauthors, 2005: The ERA-40 Re-Analysis. *Quart. J. Roy. Meteor. Soc.,* **131,** 2961–3012, doi:10.1256/qj.04.176.

Wang, B., and LinHo, 2002: Rainy season of the Asian–Pacific summer monsoon. *J. Climate,* **15,** 386–398, doi:10.1175/1520-0442(2002)015<0386:RSOTAP>2.0.CO;2.

Watanabe, T., and K. Yamazaki, 2012: Influence of the anticyclonic anomaly in the subtropical jet over the western Tibetan Plateau on the intraseasonal variability of the summer Asian monsoon in early summer. *J. Climate,* **25,** 1291–1303, doi:10.1175/JCLI-D-11-00036.1.

——, and ——, 2014: The upper-level circulation anomaly over Central Asia and its relationship to the Asian monsoon and mid-latitude wave train in early summer. *Climate Dyn.,* **42,** 2477–2489, doi:10.1007/s00382-013-1888-4.

Xiang, B., and B. Wang, 2013: Mechanisms for the advanced Asian summer monsoon onset since the mid-to-late 1990s. *J. Climate,* **26,** 1993–2009, doi:10.1175/JCLI-D-12-00445.1.

Xie, P., and P. A. Arkin, 1997: Global precipitation: A 17-year monthly analysis based on gauge observations, satellite estimates, and numerical model outputs. *Bull. Amer. Meteor. Soc.,* **78,** 2539–2558, doi:10.1175/1520-0477(1997)078<2539:GPAYMA>2.0.CO;2.

Zhang, S., and B. Wang, 2008: Global summer monsoon rainy season. *Int. J. Climatol.,* **28,** 1563–1578, doi:10.1002/joc.1659.

Zhang, Z., J. C. L. Chan, and Y. Ding, 2004: Characteristics, evolution and mechanisms of the summer monsoon onset over Southeast Asia. *Int. J. Climatol.,* **24,** 1461–1482, doi:10.1002/joc.1082.